Interactions of the Pleckstrin Homology Domain with Phosphatidylinositol Phosphate and Membranes: Characterization via Molecular Dynamics Simulations[†]

Emi Psachoulia and Mark S. P. Sansom*

Department of Biochemistry, University of Oxford, South Parks Road, Oxford OX1 3QU, U.K.

Received November 23, 2007; Revised Manuscript Received February 18, 2008

ABSTRACT: The mechanism of interaction of pleckstrin homology (PH) domains with phosphatidylinositol 4,5-bisphosphate (PIP_2)-containing lipid bilayers remains uncertain. While crystallographic studies have emphasized PH−inositol 1,4,5-trisphosphate (IP_3) interactions, biophysical studies indicate a degree of less specific protein−bilayer interactions. We have used molecular dynamics simulations to characterize the interactions of the PH domain from phospholipase C-δ1 with IP_3 and with PIP_2, the latter in lipid bilayers and in detergent micelles. Simulations of the PH domain in water reveal a reduction in protein flexibility when IP_3 is bound. Simulations of the PH domain bound to PIP_2 in lipid bilayers indicate a tightening of ligand−protein interactions relative to the PH−IP_3 complex, alongside formation of H-bonds between PH side chains and lipid (PC) headgroups, and a degree of penetration of hydrophobic side chains into the core of the bilayer. Comparison with simulations of the PH-bound domain to a PC bilayer in the absence of PIP_2 suggests that the presence of PIP_2 increases the extent of PH−membrane interactions. Thus, comparative molecular dynamics simulations reveal how a PI-binding domain undergoes changes in conformational dynamics on binding to a PIP_2-containing membrane and how interactions additional to those with the PI headgroup are formed.

Many cellular processes, including cytoskeletal organization, signaling, and membrane trafficking, involve lipid–protein interactions (*1*). During these processes, cytoplasmic proteins interact with cellular membranes. Such proteins are known as peripheral proteins, and most of them contain one or more modular domains for binding specific ligands in cell membranes [see http://proteomics.bioengr.uic.edu/metador/MeTaDoR.html (*2*) for a useful summary]. A key membrane-interacting domain is the pleckstrin homology (PH)[1] domain (*3*).

The PH domain contains 100−120 amino acids and is perhaps the most common membrane-targetting domain (*4*). Many PH domain-containing proteins are implicated in cellular signaling mechanisms which require association with the cell membranes by binding to specific lipid molecules (*5*). However, despite the widespread occurrence of this domain, it is not clear that it has a single function, as only 10% of PH domains bind phosphoinositides tightly (*3*). Structures for the PH domain are known from 13 different proteins (*4*), including spectrin (*6*), dynamin (*7*), and phospholipase C-δ1 (PLCδ1) (*8*). Although they have a relatively low degree of sequence homology, all the PH domains share a similar fold, containing two orthogonal antiparallel β-sheets (of three and four strands, respectively) followed by a C-terminal α-helix (Figure 1) (*1*).

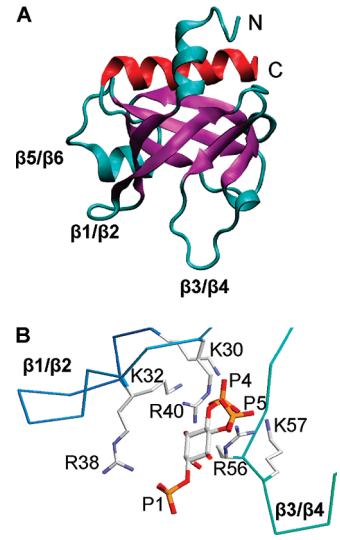

FIGURE 1: X-ray structure of the PLCδ1 PH domain. (A) The fold shown in ribbon format with the two orthogonal antiparallel β-sheets colored purple and the C terminal α-helix colored red. The three loops which form the membrane interaction surface are labeled. (B) Bound IP3 molecule, showing the key basic side chains (see the text for details) which interact with the phosphates.

Phosphoinositides (PIs) are polyanionic headgroup lipids involved in phosphorylation events as signal mediators, in membrane trafficking, and in nuclear events, etc. (*5, 9, 10*). They also interact with a number of integral membrane proteins such as ion channels (*11*). Differential patterns of phosphorylation at positions 3, 4, and 5 on the inositol ring

[†] Research in M.S.P.S.'s laboratory is supported by the BBSRC, the EPSRC, and the Wellcome Trust. E.P. was supported by a Wellcome Trust Structural Biology studentship.

* To whom correspondence should be addressed. Phone: +44-1865-275371. Fax: +44-1865-275273. E-mail: mark.sansom@bioch.ox.ac.uk.

[1] Abbreviations: CG, coarse-grained; DPC, dodecylphosphocholine; DPPC, dipalmitoylphosphatidylcholine; IP_3 or Ins(1,4,5)P_3, inositol 1,4,5-trisphosphate; MD, molecular dynamics; PC, phosphatidylcholine; PH, pleckstrin homology; PI, phosphoinositide; PIP_2 or PI(4,5)P_2, phosphatidylinositol 4,5-bisphosphate; PME, particle mesh Ewald; rmsd, root-mean-square deviation; rmsf, root-mean-square fluctuation.

10.1021/bi702319k CCC: $40.75
Published on Web 03/15/2008

can generate seven distinct PIs. Understanding the details of the PI−protein interactions is important for potential therapeutic applications as misreading of the PI signals has been implicated in a number of disorders (*12–15*).

The most abundant PI is phosphatidylinositol 4,5-bisphosphate [$PI(4,5)P_2$], to which the PH domain of phospholipase Cδ1 (PLCδ1) binds with high affinity (*16, 17*). PLCδ1 belongs to a family of 13 inositol phospholipid-specific phospholipase C (PLC) isozymes that are divided into six classes (*18, 19*). The PLCδ subfamily is activated by high calcium levels and by binding to $PI(4,5)P_2$ through its PH domain (*20, 21*). PLCδ1 consists of an N-terminal PH domain (*8*), followed by an EF-hand domain, a catalytic domain, and a C-terminal C2 domain (*22*).

The structure of the PH domain from rat phospholipase C-δ1 bound to $Ins(1,4,5)P_3$ [the headgroup of the lipid $PI(4,5)P_2$] has been determined by X-ray crystallography to 1.9 Å resolution [Protein Data Bank (PDB) entry 1MAI] (*8*). In this structure, the $Ins(1,4,5)P_3$ ligand forms hydrogen bonds to nine different residues of the protein, namely, K30, K32, W36, R40, E54, S55, R56, K57, and T107, with R38 in the proximity (*8*). These are located primarily on the $\beta1-\beta2$ and $\beta3-\beta4$ loops of the PH domain. In addition to these interactions, positively charged residues of the $\beta1-\beta2$ and $\beta3-\beta4$ strands and loops have been suggested to form contacts with the phospholipid headgroups of the membrane (*23*).

There is currently some debate about whether regions other than the IP_3-binding site contribute to the interactions of the PH domain with membranes. As discussed in, for example, ref *1*, for many PI-binding proteins, specific lipid binding results in nonspecific membrane penetration of the protein. However, these authors suggest that this is not the case for PH domains, and it has been noted that the PLCδ1 PH domain binds more weakly to PIP_2 in membrane vesicles than to isolated IP_3 (*8, 17*). This argues against a nonspecific interaction. In contrast, several recent studies (*24–26*) suggest nonspecific PH−membrane interactions may be important. In particular, it has been shown that PLCδ1 PH can insert into lipid monolayers in the absence of PIP_2 and that such interactions are enhanced by the presence of anionic lipids in the monolayer (*26*).

Given that the interactions of membrane proteins with their environment are intrinsically dynamic, molecular dynamics (MD) simulations (*27*) have played a key role in developing our understanding of integral membrane proteins (*28*) and their function (*29*). More recently, MD simulations have been used to investigate the nature of the interactions of a number of peripheral proteins with phospholipid bilayers (*30–35*).

In this paper, we compare MD simulations of the PLCδ1 PH domain in three different environments, i.e., in water, in a DPC micelle, and in a DPPC bilayer. This enables us to study both specific PH−PIP_2 and nonspecific PH−lipid (and PH−detergent) interactions. We address two key questions, namely, the influence of ligand and environment on the conformational dynamics of a PH domain and the possible role of interactions with the lipids of a bilayer membrane. Our simulations provide evidence indicating that the PH domain will interact with a bilayer interface in the absence of PIP_2 but that the presence of PIP_2 increases the extent of PH−membrane interactions.

METHODS

Simulations. The GROMACS 3.0 simulation package (www.gromacs.org) (*36, 37*) was used for all simulations, with a united atom GROMOS96 force field (*38*) and the SPC water model (*39*). Periodic boundary conditions were applied to the systems. Long-range electrostatics were calculated using the PME (particle mesh Ewald) method (*40, 41*) with a real-space cutoff of 10 Å. For the van der Waals interactions, a cutoff of 10 Å was used. The Apo, IP3, and Mic simulations were performed at 300 K and the Bil and Apo/Bil simulations at 323 K, using a Berendsen thermostat (*42*) with a coupling constant τ_T of 0.1 ps. A constant pressure of 1 bar was maintained using a Berendsen barostat with an isotropic coupling constant τ_P of 1.0 ps and a compressibility of 4.5×10^{-5} bar^{-1}. The integration time step for the Apo simulations and the IP3 simulations was 2 fs and for the Mic, Bil, and Apo/Bil simulations 1 fs. The LINCS method (*43*) was used to constrain bond lengths. Coordinates were saved every 5 ps for analysis. Analysis of all simulations was performed using the GROMACS package. Docking used Autodock version 3.05 (*44*). VMD (*45*), PyMol (www.pymol.org), and RasTop [http://sourceforge.net/projects/rastop/ (*46*)] were used for visualization.

PLCδ1 PH Domain Structure. The X-ray structure of the pleckstrin homology (PH) domain from rat phospholipase C-δ1 (PDB entry 1MAI; resolution of 1.9 Å) was used as the starting structure for all the simulations. In this, the PLCδ1 PH domain is bound to $Ins(1,4,5)P_3$. It was assumed that all ionizable residues were in their standard charge state at neutral pH, yielding a net charge of $+2e$. The protein structure was energy-minimized using 100 steps of steepest descent in vacuo prior to simulation setup.

$Ins(1,4,5)P_3$ and $PI(4,5)P_2$ Structures. $Ins(1,4,5)P_3$ was modified from the X-ray structure in 1MAI using InsightII (http://www.accelrys.com/products/insight/index.html) to add the missing hydrogens to the inositol molecule. Its topology for GROMACS was obtained using PRODRG (*47*), yielding to total charge of −5e (cf. ref *48*). The $Ins(1,4,5)P_3$ model structure was then energy-minimized and tested via a 2 ns simulation in water (subsequently extended to 10 ns). The $PI(4,5)P_2$ structure was constructed by fitting the $Ins(1,4,5)P_3$ headgroup to a dipalmitoylglycerol moiety. As before, the topology for $PI(4,5)P_2$ was generated using PRODRG. The $PI(4,5)P_2$ model structure was energy-minimized and tested via a 1 ns simulation of the lipid in water.

Simulation Systems. Five simulations of the PLCδ1 PH domain were performed: Apo, IP3, Mic, Bil, and Apo/Bil (Table 1). In the Apo simulation, the PH domain was solvated with 4432 SPC water molecules and two Cl^- ions were added at random locations within the simulation box (with dimensions of 56 Å × 58 Å × 46 Å) to neutralize the protein charge. The system was then energy-minimized and the simulation run for 10 ns. In the IP3 simulation, the PH domain was bound to $Ins(1,4,5)P_3$. The complex was solvated with 5595 waters, and three Na ions were added. The system (box with dimensions of 60 Å × 62 Å × 50 Å) was energy-minimized and the simulation run for 10 ns.

The Mic simulation was of the PH domain bound to a single $PI(4,5)P_2$ molecule pre-embedded in a DPC micelle. The DPC micelle was generated by a self-assembly simulation, as described previously (*49*). $PI(4,5)P_2$ was added to a

Table 1: Summary of Simulations

simulation	system	no. of atoms	duration (ns)	Cα rmsd[a] (Å)	core Cα rmsd[b] (Å)
Apo	PLCδ1 PH + 4432 waters	14570	10	2.6	1.3
IP3	PLCδ1 PH + Ins(1,4,5)P_3 + 5595 waters	18087	10	1.8	1.2
Mic	PLCδ1 PH + PI(4,5)P_2 + 54 DPCs + 13630 waters	43474	30	2.1	1.5
Bil	PLCδ1 PH + PI(4,5)P_2 + 248 DPPCs + 16480 waters	63185	20	1.7	1.4
Apo/Bil	248 DPPCs +16478 waters	63108	15	1.4	1.1

[a] The value given is for all residues, averaged over the final 2.5 ns of the two 10 ns simulations, and over the final 5 ns of the 15, 20, and 30 ns simulations. [b] The value given is for the residues of the core fold (i.e., excluding surface loops).

DPC micelle via replacement of one of the DPC molecules to yield a mixed micelle containing one PI(4,5)P_2 and 54 DPC molecules. This was energy-minimized before the protein was added by superimposition of the IP3 molecule (subsequently discarded) on the headgroup of the PIP_2. The protein/micelle system was solvated with 13630 water molecules, and three Na^+ ions were added. The whole system (box with dimensions of 77 Å × 80 Å × 75 Å) was energy-minimized and the system run for 30 ns.

The Bil simulation was of the PH domain bound to PI(4,5)P_2 in a DPPC bilayer. A pre-equilibrated DPPC bilayer was generated as described previously (*50*). PI(4,5)P_2 was added to a DPPC bilayer via replacement of one of the lipids to yield a single PIP_2 in a bilayer of 248 DPPC lipids. This was energy-minimized, and then the protein was added (again via superimposition of IP_3 on the PIP_2 headgroup). The protein/bilayer system was solvated with 16480 water molecules, and three Na^+ ions were added, yielding a simulation box with dimensions of 105 Å × 90 Å × 100 Å. The resultant system was energy-minimized, and then a simulation was run for 0.2 ns with isotropic position restraints on the non-H atoms of the PH domain and of PI(4,5)P_2 followed by a further 0.2 ns with restraints on the *z*-coordinates only, to allow water and DPPC molecules to relax around the protein−PIP_2 complex. Finally, all restraints were removed, and the production simulation was run for 20 ns.

For the Apo/Bil simulation, the PIP_2 molecule was removed from the Bil system after the protein-restrained equilibration, and the three Na^+ ions were removed and two Cl^- ions added to yield a neutral system. The resultant system was then energy-minimized and a further equilibration run for 0.2 ns with isotropic position restraints on the non-H atoms of the PH domain. Finally, all restraints were removed, and the unrestrained simulation was run for 15 ns.

A preformed DPC micelle was generated as described previously (*51*) using 55 DPC molecules. This corresponds to the aggregation number of DPC micelles suggested by ref *52*. The DPPC bilayer was generated as described previously (*50*).

Coarse-Grained Simulations. Coarse-grained (CG) simulations were performed using the Marrink CG force field (*53*), in which one particle represents approximately four non-H atoms, modified as described in refs *54–56* to include proteins. A DPPC bilayer and a DPC micelle were generated by self-assembly CG simulations, starting from either 256 DPPC lipid molecules or 29 DPC detergent molecules randomly positioned in a simulation box. Subsequently, the PH domain was positioned in the simulation box a suitable distance (~20 Å) from the preformed DPPC bilayer or DPC micelle, and water particles were added. Note that PIP_2 was not included in the CG simulations. Multiple simulations ~2 μs in duration were performed for each system.

RESULTS

Simulations in Different Environments. To explore the relationship among environment, conformational dynamics, and PIP_2 binding, five simulations of the PLCδ1 PH domain were performed, as summarized in Table 1. Thus, the IP3 and Apo simulations compare the PH domain in water (i.e., in the absence of a membrane), with and without bound Ins(1,4,5)P_3, respectively. We have also performed two simulations in which the PH domain is bound to a PI(4,5)P_2 molecule which is embedded in either a simple phospholipid bilayer or a detergent micelle. The latter simulation was included as micelles have been used in a number of studies of PI-interacting domains, e.g., enzymatic assays of PLCδ1 (*57*) and NMR studies of protein−PI interactions of FYVE domains (*58*), and have been used to generate models of domain−membrane interactions (*59*). Finally, we performed a simulation in which the PH domain not bound to PI(4,5)P_2 is embedded in a phospholipid bilayer. The behavior of the PH domain in the two bilayer simulations will be then compared, and hence, we can examine the influence of the binding to PI(4,5)P_2 on the interactions of the PH domain with membrane lipids.

The details of the setup of the simulations are described in Methods. From the overall root-mean-square deviations (rmsds) of the Cα atoms from the initial (X-ray) coordinates, it is evident that the protein is globally stable in all five simulations. However, it is also clear that the presence or absence of bound IP_3, PI(4,5)P_2, or a lipid bilayer influences the degree of conformational drift of the PH domain. Furthermore, there are small but significant differences in conformational drift for the liganded protein in different environments. These differences are explored in more detail below.

PLCδ1 PH Domain in Water. The conformation drift of the isolated PH domain in water with and without bound Ins(1,4,5)P_3 was assessed from the comparison Cα rmsds of the IP3 and Apo simulations, respectively (Figure 2A). There is a clear difference between the two simulations. In the IP3 simulation, the domain is conformationally quite stable: after an initial rise (typical for protein simulations), the overall Cα rmsd remains constant at ~1.8 Å. In contrast, in the Apo simulation, the overall Cα rmsd shows a more complex behavior. For the first ~3 ns, it is approximately constant at ~1.8 Å, i.e., similar to the IP3 simulation. There is then a jump in the rmsd to a higher value (~3 Å). Visualization of the simulation suggests that this transition corresponds to changes in the conformation of the β3−β4 and β5−β6 loops, which moved away from the core fold.

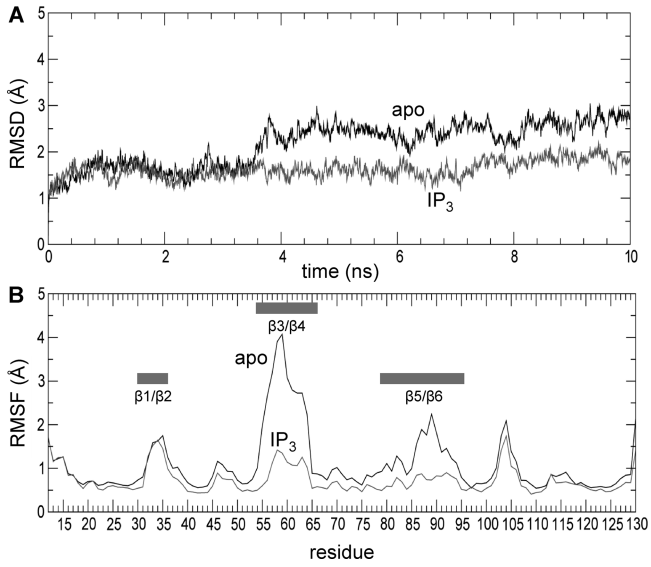

FIGURE 2: Apo and IP3 simulations. (A) The Cα rmsds relative to the starting structure are shown as a function of time for the Apo (black line) and IP3 (gray line) simulations. (B) Cα rmsf profiles (i.e., rmsf vs residue number) for the Apo (black line) and IP3 (gray line) simulations.

Indeed, there is little difference between the two simulations in rmsds for the residues of the core fold (i.e., excluding loops) of the protein (Table 1). Thus, overall, it seems that the PH domain exhibits greater conformational drift in the absence of bound ligand; i.e., the presence of a bound ligand stabilizes the conformation of the protein. This has been observed for a number of other proteins (*60*).

The relatively low Cα rmsd in the IP3 simulation may be related to the relatively high resolution of the protein structure (1.9 Å). Similar values have been observed in simulations based on a number of other high-resolution protein structures (E. Psachoulia, M. S. P. Sansom, and P. Biggin, unpublished data; also see ref *61*). This strengthens our confidence in the significance of the greater degree of conformational drift seen in the Apo simulation.

To investigate further the origin of the higher rmsd in the Apo simulation, the Cα atom rmsf profiles (as a function of residue number) were calculated for both simulations (Figure 2B). The overall forms of the two profiles are as anticipated, with lower rmsfs for core secondary structure elements and higher rmsfs for surface loops. There is, however, a clear difference between the Apo and IP3 simulations, namely markedly higher rmsfs for the $\beta3-\beta4$ and $\beta5-\beta6$ loops in the Apo simulation than in the presence of IP_3. This is significant because the residues in the $\beta3-\beta4$ loop region (e.g., K57) play a role in IP_3 binding and the presence of IP_3 reduces the flexibility of the $\beta5-\beta6$ loop.

The interactions of basic side chains with the phosphates of IP_3 have been suggested to be the key to ligand binding by PH domains (*3*). These interactions were analyzed by monitoring basic side chain−phosphate distances in the IP3 simulation (Figure 3). As anticipated, the P4 and P5 phosphates form tighter interactions than P1. Thus, P5 forms three salt bridges throughout the simulation, and P4 fluctuates between two and three salt bridges, the K32−P4 salt bridge being broken during the simulation. In contrast, P1 forms fewer than one weak salt bridge on average (to R38). Visual comparison of the IP3 simulation with the X-ray structure

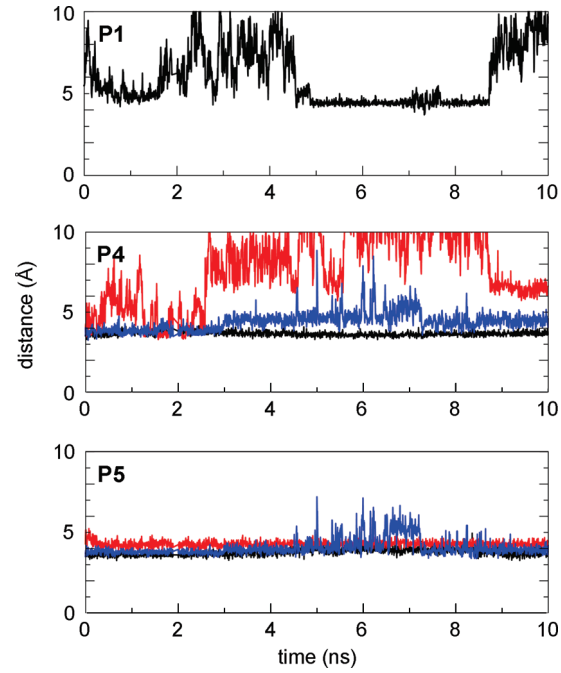

FIGURE 3: Side chain−phosphate distances for the IP3 simulation. Distances between the phosphorus atom and the NZ (for lysines) or CZ (for arginines) atoms of interacting basic residues for the IP3 simulations. The following distances are shown: P1−R38 (black); P4−K30 (black), P4−K32 (red), and P4−K57 (blue); and P5−K30 (black), P5−R40 (red), and P5−K57 (blue).

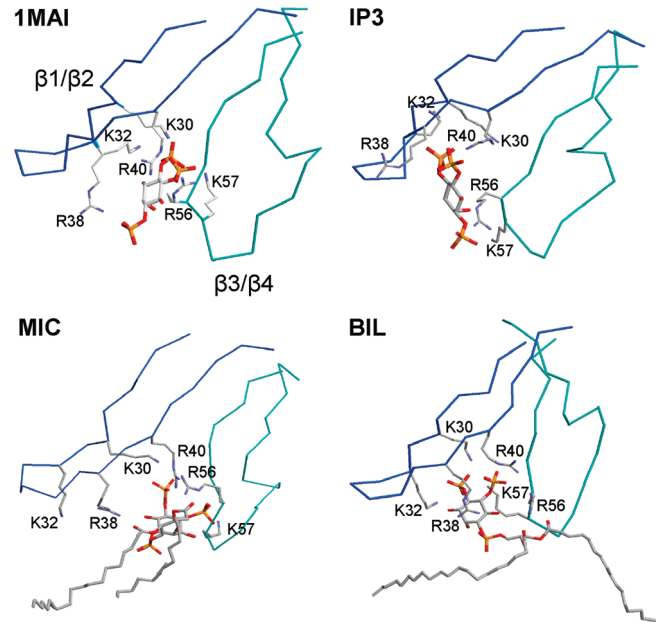

FIGURE 4: Comparison of ligand binding interactions. The ligand−basic side chain interactions are shown for 1MAI (the X-ray structure), IP3 (the IP3 simulation at 10 ns), MIC (the Mic simulation at 30 ns), and BIL (the Bil simulation at 20 ns).

indicates some degree of flexibility in the orientation of IP3 at the binding site (Figure 4). This is perhaps not surprising given the likely flexibility of the long side chains (lysine and arginine) forming the main interactions to the (also themselves flexible) phosphates of the ligand.

As noted above, one of the loops contributing to the IP3 binding site ($\beta3-\beta4$) was quite flexible in the Apo simulation. We examined the possible functional consequences of this via docking of IP_3 to simulation snapshots, namely to

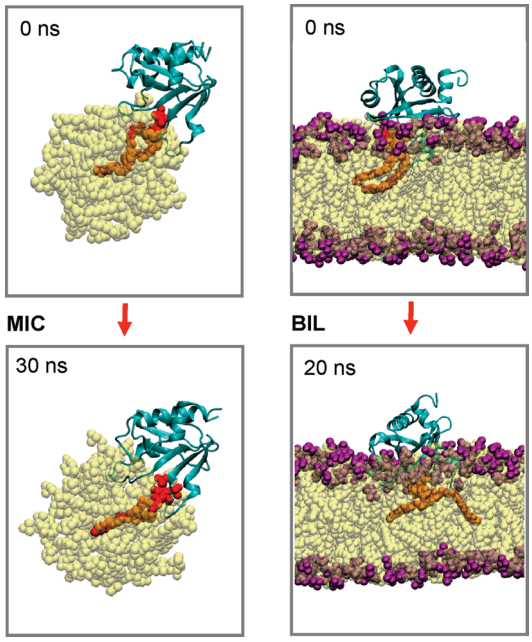

FIGURE 5: PH domain−micelle and PH domain−bilayer interactions. Snapshots are shown at the start of the Mic and Bil simulations (i.e., at 0 ns) and at the end of each simulation. The protein is in cyan ribbon format. The DPC molecules are in yellow van der Waals format. The DPPC molecules are colored yellow with headgroups colored purple. PI(4,5)P_2 is colored red and orange.

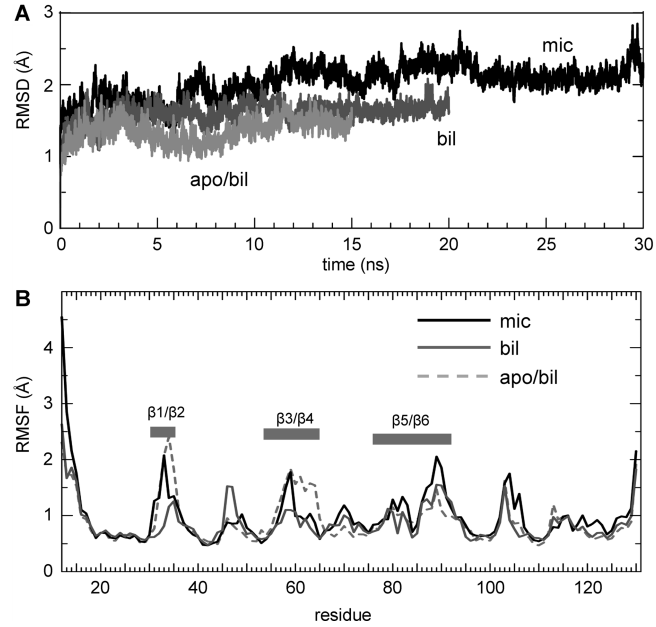

FIGURE 6: Mic and Bil simulations. (A) The Cα RMSDs relative to the starting structure are shown as a function of time for the Mic (black line), Bil (dark gray line), and Apo/Bil (light gray line) simulations. (B) Cα rmsf profiles (i.e., rmsf vs residue number) are shown for the Mic (black line), Bil (solid gray line), and Apo/Bil (dashed gray line) simulations.

four representative structures generated by clustering (on Cα rmsds) of the Apo trajectory. For three of the four structures, IP_3 was successfully docked to a site made up of residues from both the $\beta1-\beta2$ and $\beta3-\beta4$ loops; for one structure, only the $\beta1-\beta2$ residues interacted with the docked IP_3. This suggests that despite the enhanced flexibility in the Apo simulation, the ligand-binding site remained functionally intact.

PLCδ1 PH Domain in Membranelike Environments.

(1) The Simulations. We also analyzed the interactions of a PH domain with PIP_2 in a membranelike environment, rather than with an isolated IP_3 molecule in water. Toward this end, we generated two membranelike systems (Figure 5): one with a single PIP_2 molecule embedded in a detergent micelle (Mic simulation) and the other with a PIP_2 molecule in a phospholipid bilayer [Bil simulation (Table 1)]. We note that the latter system is similar to that used by Tuzi et al. (*25*) in solid-state NMR studies of the PLCδ1 PH domain bound to PIP_2 in a PC bilayer. In both cases, the initial configuration of the simulation system was generated by fitting the IP_3 molecule in the X-ray structure of the PH−IP_3 complex onto the corresponding headgroup of a PIP_2 in a micelle or bilayer, thus retaining the (fitted) protein coordinates and the pre-equilibrated micelle or bilayer plus PIP_2 coordinates as the starting model for the subsequent simulation (see Methods for further details). We also performed a control simulation (Apo/Bil) of the PH domain bound to a PC bilayer in the absence of PIP_2.

Visualization of the structures at the start and end of the simulations (Figure 5) suggests that in both cases the PIP_2 remains tightly bound between the $\beta1-\beta2$ and $\beta3-\beta4$ loops, while additional regions of the protein surface interact with the micelle or bilayer surface. In particular, there seems to be a "deeper" insertion of the PH domain into the bilayer−water interfacial region than into the micelle. Both classes of interaction, specific and nonspecific, are examined in more detail below.

(2) Conformational Drift and Flexibility. As before, conformational drift was assessed via measurement of Cα rmsd values relative to the initial (X-ray) structure for each simulation (Figure 6A). In both cases, the rmsd underwent an initial rise. For the Mic simulation, there were subsequently relatively small fluctuations about the 2 Å value for the remainder of the 30 ns simulation. For the Bil simulation, there was an increase at ~3 ns to ~1.7 Å and it remained at this same value during the 20 ns simulation. The final rmsd value of the Bil simulation was thus significantly lower than for the Mic simulation, but approximately the same when the surface loops were excluded from this analysis (Table 1). Thus, in the bilayer simulation, the loops seem to change conformation less than in the micelle simulation, despite a greater degree of penetration (see below) into the bilayer.

Examination of the Cα rmsf profile simulations (Figure 6B) and comparison with that for the IP3 simulation reveal some interesting features. For the Mic and Bil simulations, the overall pattern of rmsfs was similar to that seen in the IP3 simulations, with low rmsfs for residues in the β-strands and α-helices and higher values for residues in the loops. The only major difference between the IP3 simulation and the Mic/Bil simulations is that the rmsf in the $\beta5-\beta6$ region (which includes helix α2) is somewhat higher for the latter. As we will see, this is a region which interacts with the detergent and lipid molecules and which is observed to undergo membrane-induced changes in conformation in solid-state NMR studies (*25*). Moreover, the rmsf profile for the Apo/Bil simulation is similar to the profiles for the Mic and Bil simulations. The rmsf values in the $\beta5-\beta6$ region are the same as in the Bil simulation, but significantly, in the $\beta1-\beta2$ and $\beta3-\beta4$ regions involved in PI(4,5)P_2 binding, the rmsf values are somewhat higher than in the Bil simulation. This suggests that the presence of bound PI(4,5)P_2

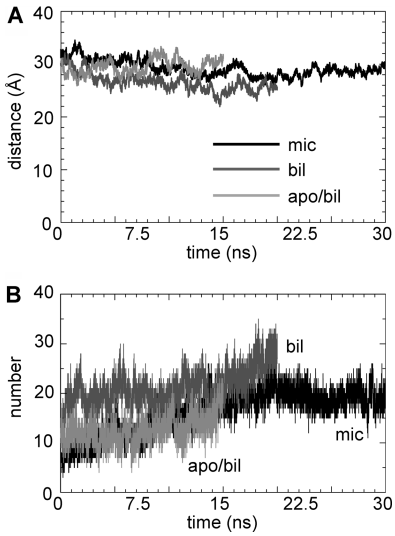

FIGURE 7: Insertion of the PH domain into the micelle or bilayer. (A) Distance between the center of mass of the PH domain and the center of mass of the DPC micelle (Mic, black line) or of the DPPC bilayer (Bil, dark gray line; and Apo/Bil, pale gray line). (B) Number of hydrogen bonds between the PH domain and the detergents or lipids for the Mic (black line), Bil (dark gray line), and Apo/Bil (light gray line) simulations.

reduces the flexibility of these loops, although the differences are less pronounced than those between the Apo and IP3 simulations (see above). However, it is interesting to note that when a micelle or a bilayer is present, the flexibility of the $\beta5-\beta6$ loop is higher than in the IP3 simulation. This was unexpected and is presumed to reflect the additional interactions with the detergent or lipid molecules. The flexibility of this loop in the micelle simulation [rmsf $\sim$ 2 Å, which is still less than in the Apo simulation (rmsf $\sim$ 2.3 Å)] is somewhat higher than that in the Bil and Apo/Bil simulations (both rmsfs $\sim$ 1.5 Å). This may reflect differences in headgroup mobility between the detergent and lipid molecules. We note that previous simulations of an integral membrane protein had suggested somewhat enhanced flexibility in the micelle relative to the bilayer environment (*51*).

(3) Protein−Environment Interactions. As mentioned above, visualization of the Mic and Bil simulations (Figure 5) suggests in both cases the protein forms additional protein−lipid contacts during the course of the simulation, with some degree of insertion of protein residues into the micelle or bilayer. This is particularly evident for the Bil simulation in which the PH domain penetrates into the headgroup−water interface of the bilayer. Similarly, in both of these simulations, a decrease in the total number of protein−water H-bonds (from ~280 and ~250 at the start of the simulations to ~260 and ~230 at the end of the Mic and Bil simulations, respectively) was observed. By way of comparison, in, e.g., the Apo simulation, the total number of H-bonds to water was constant at 286 ± 11 throughout the simulation.

To further characterize the degree of insertion of the PLCδ1 PH domain into the micelle and the bilayer, the distance of the center of mass of the PH domain from the center of mass of the micelle detergents or bilayer lipids was calculated as a function of simulation time (Figure 7A). For the Mic simulation, this distance decreased from ~32 Å at the start of the simulation over the first ~10 ns and then remained at ~29 Å for the remainder of the simulation. We checked that this apparent increase in the depth of penetration of the micelle did not simply reflect a change in the micelle geometry. Thus, the radius of gyration of the micelle was ~17 Å over the first 20 ns of the simulation and was ~20 Å over the final 10 ns. The radius of gyration of the PH domain was constant at 14 Å throughout the simulation. Thus, summing the two radii of gyration and comparing them with the distance between the centers of mass of the detergent and protein, we can see that some degree of insertion of the protein into the micelle occurs during the simulation. In the Bil and Apo/Bil simulations, the distance of the center of the PLCδ1 PH domain from the center of the DPPC bilayer along the *z*-axis (i.e., the bilayer normal) was initially ~31 Å. Note that each bilayer leaflet is ~25 Å thick. In the Bil simulation, this distance decreased rapidly to ~27 ± 1 Å at ~5 ns and more slowly to 25 ± 1 Å (averaged over the last 5 ns) at the end of the simulation. Thus, the PH domain inserted to a small degree into the DPPC bilayer early in the simulation and remained there. In contrast, in the Apo/Bil simulation, there was no sustained decrease in the distance but rather it fluctuated between 26 and 31 Å, suggesting a weaker interaction of the PH domain with the bilayer lipids when the PH domain was not bound to $PI(4,5)P_2$. In summary, in all cases, this analysis suggests significant nonspecific interaction between the micelle or bilayer and the PH domain.

(4) Interactions with PIP_2. We characterized in detail the interactions of the PLCδ1 PH domain with PIP_2 when the protein was in a membrane environment. From analysis of the residues forming the closest contacts to PIP_2 during the Mic and Bil simulations [cutoff of 6 Å (data not shown)], it was found that for the Mic simulation the residues closest to the PIP_2 were K30, W36, R38, R40, Q53, S55, R56, and K57. For the Bil simulation, the residues close to PIP_2 were largely the same as in the Mic simulation, namely, K30, K32, W36, R38, R40, Y42, S55, R56, K57, and V58.

From this preliminary analysis, it was evident that, as in the IP3 simulation, contacts between basic side chains and phosphate groups played a key role in interactions of the PH domain with PIP_2 (Figure 8). Focusing on these interactions, we see that, for the Mic simulation, the P1 phosphate forms a weak interaction with R38. In contrast, both P4 and P5 form tighter interactions. Thus, P4 initially interacts with the side chains of K32 and K30. At ~2 ns, a switch occurs such that the K32−P4 interaction is broken and the K30−P4 interaction is weakened, while K57 forms a tight interaction which replaces K32. For P5, there is an interaction with K30 throughout the simulation while the R40 and K57 interactions fluctuate. Overall, the simulations suggest a dynamic and/or flexible interaction for PH interacting with PIP_2 in a micellar environment.

A comparable, but somewhat tighter, pattern of interactions is seen in the Bil simulation. Thus, P4 interacts with K30, K32, and K57 throughout the simulation, alongside intermittent weaker interactions with R56. Similarly, for P5, the interactions with K30, R40, and K57 are present throughout the simulation, while that with R56 fluctuates. Interestingly, for P1, there is an interaction with R56 (which bridges the P1 phosphate and the lipid acyl and glycerol groups) and (more distantly) with R38 (which also bridges the acyl groups of PIP_2). Thus, on balance, the interactions of PH domain basic side chains and PIP_2 phosphates seem to be tighter

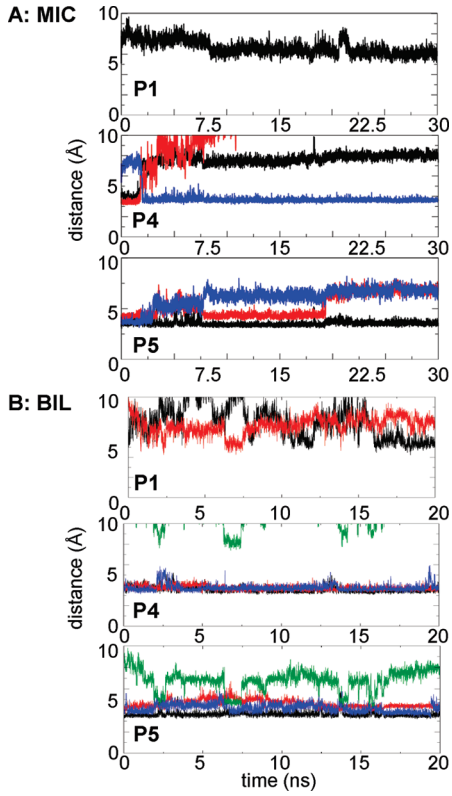

FIGURE 8: Side chain−phosphate distances for the Mic and Bil simulations. Distances between the phosphorus atom and the NZ (for lysines) or CZ (for arginines) atoms of interacting basic residues for the IP_3 simulations. For the Mic simulation, the following distances are shown: P1−R38 (black); P4−K30 (black), P4−K32 (red), and P4−K57 (blue); and P5−K30 (black), P5−R40 (red), and P5−K57 (blue). For the Bil simulation, the following distances are shown: P1−R38 (black) and P1−R56 (red); P4−K30 (black), P4−K32 (red), P4−K57 (blue), and P4−R56 (green); and P5−K30 (black), P5−R40 (red), P5−K57 (blue), and P5−R56 (green).

(i.e., closer and longer-lasting) for the bilayer environment. This may be related to the smaller degree of conformational drift of the protein structure in the Bil than in the Mic simulation (see above). Indeed, the interaction in the Bil simulation is also tighter than in the IP3 simulation.

(5) Nonspecific Interactions with Lipids and Detergents. To examine further the (nonspecific) interactions with lipid or detergent molecules, we determined the overall numbers of H-bonds between lipid or detergent molecules and protein (Figure 7B). For all simulations, these increased slowly over the first 5–10 ns, eventually reaching plateau values such that Bil > Mic > Apo/Bil in terms of the number of H-bonds to lipid (or detergent). Thus, in all simulations, the PH domain forms significant H-bonding contacts with the headgroups of the lipid or detergent molecules, but these seem to be greatest in number for the PH domain bound to PIP_2 in a bilayer.

A general analysis of protein residues in close (cutoff of 6 Å) contact with lipid or detergent molecules revealed three main regions to be involved: $\beta1-\beta2$, $\beta3-\beta4$, and $\beta5-\beta6$ loops [which includes the amphipathic α2 helix (Figure 9)] form significant contacts. In addition, in the Bil simulation, the $\beta6-\beta7$ loop formed contacts (Figure 9B). This is in broad agreement with biochemical (*24*) and solid-state NMR (*25*) studies. Thus, using a combination of chimeric proteins and mutagenesis (*24*), it was shown that the $\beta6-\beta7$ loop, in addition to the PIP_2 binding site region, was a critical

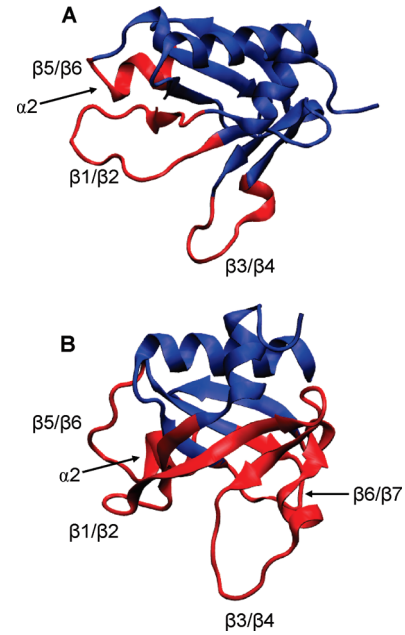

FIGURE 9: Regions of the PH domain interacting with lipids or detergents. Residues of the PH domain which interact with detergent (A for the Mic simulation) or lipid (B for the Bil simulation) molecules are colored red. The loops, and the α2 helix (part of the $\beta5-\beta6$ loop), which form nonspecific contacts with the micelle (A) or bilayer (B) are indicated.

component for membrane localization of the PLCδ1 PH domain in intact cells. Significantly, this is the additional loop which interacts with lipid in the Bil simulation. In the NMR study (conducted using a phosphatidylcholine bilayer) (*25*), the contacts suggested were in the $\beta5-\beta6$ loop and in the amphipathic α2 helix. This again correlates well with the simulation studies.

A more detailed analysis of the residues of the PH domain interacting with the lipid headgroups in the Bil simulation revealed that just 16 residues (in the $\beta1-\beta2$ loop residues S33, S34, S35, R37, R38, and R40; in the $\beta3-\beta4$ loop residues Q53, R56, K57, S61, and S64; in helix α2 residues K86 and R89; and in the $\beta6-\beta7$ loop residues Q104, R105, and N106) formed 75% of the hydrogen bonds of the domain with the DPPC bilayer. It was also seen that approximately six residues located at the $\beta3-\beta4$ loop interacted with the nonpolar atoms of the DPPC lipids during the last 5 ns of the simulation. Furthermore, residue W36 interacted with both polar and the nonpolar regions of the lipids. Thus, both polar and nonpolar nonspecific interactions are formed between the PH domain and its lipid bilayer environment.

(6) Coarse-Grained Simulations of Nonspecific Interactions. It is important to evaluate the extent to which the simulations reported here (with a duration of ~20 ns) provide a meaningful sample of protein−bilayer interactions. This is especially the case as it is known that substantially longer simulation times are needed to fully sample protein dynamics in atomistic membrane protein simulations (*62*). Furthermore, insertion of a peptide into a bilayer requires simulation times of ~500 ns (*63*). However, simulations of a number of membrane-interacting domains [e.g., H-Ras (*64*), cPLA2-C2 (*34*), and GLA (*65*)] on a 10–30 ns time scale have yielded meaningful information about protein−bilayer interactions, and so we have some confidence in the value of the studies presented here. Nevertheless, it is helpful to have

another measure of PH domain−bilayer interactions. To achieve this, we have exploited recent developments in coarse-grained molecular dynamics (CG-MD) simulations of membrane proteins (*54–56, 66, 67*) to explore nonspecific PH−lipid interactions.

To this end, 2 μs duration CG-MD simulations of the PH domain were performed in two different environments: a detergent (DPC) micelle and a lipid (DPPC) bilayer. In neither case was PIP_2 present. In both cases, within ~0.8 μs the PH domain bound to the micelle or bilayer and remained bound for the rest of the simulation. In all of the CG-MD simulations, the main regions of the PH domain which interacted with the detergent or the lipid molecules were the same as in the atomistic simulations, i.e., the $\beta1-\beta2$, $\beta3-\beta4$, $\beta5-\beta6$, and $\beta6-\beta7$ loops. The only difference between the CG and AT simulations was that some residues of the $\beta7$ strand and the beginning of the C-terminal α-helix additionally interacted with lipid molecules in the CG simulations. We note that the C-terminal α-helix has been implicated in membrane contacts in some experimental studies (*24*).

In the CG simulations of the interaction of the PH domain with a DPPC bilayer (which were initiated with the PH domain away from the bilayer at a center−center distance of 60 Å), the final distance between the center of mass of the PH domain and that of the bilayer was 30 Å. This compares well with the value of ~25 Å for the atomistic simulations, especially when the difference in "resolution" between the atomistic and CG simulations is taken into account. Therefore, the degree of agreement between the CG and atomistic simulation results provides persuasive evidence of the latter in terms of the global location of the PH domain relative to the bilayer or micelle.

DISCUSSION

On the basis of the simulation results presented above, it is possible to suggest a tentative mechanism for the interaction of the PH domain of PLC$\delta1$ with PIP_2 in a membrane, which extends the view derived from the X-ray structure (*7*) and which is supported by, for example, recent solid-state NMR data (*25, 68*). In this model, specific interactions between the PH domain and ligand reduce binding site flexibility, while nonspecific interactions between the protein and lipid enable a degree of bilayer penetration by the domain.

The Apo state of the PH domain appears to be relatively flexible in the region of the $\beta3-\beta4$ and $\beta5-\beta6$ loops. This is relevant to PI binding as residues R56 and K57 are on the $\beta3-\beta4$ loop (the other basic residues are on the $\beta1-\beta2$ loop). We note that a change in binding site loop mobility upon IP_3 binding has been seen in NMR studies of the spectrin PH domain (*69*).

When the PH domain binds to the IP_3 headgroup of PIP_2, there appears to be a degree of restriction of the protein mobility. Furthermore, the R56 side chain (which points away from IP_3 in the X-ray structure) forms a bridge from the P1 phosphate to the acyl/glycerol region of the PIP_2 molecule throughout the bilayer simulation. The R38 side chain forms a fluctuating interaction with P1 and with the acyl group of the PIP_2. In addition to this tightened interaction with PIP_2, there also seem to be nonspecific H-bonding interactions of surface residues of the PH domain with lipid headgroups, and some limited degree of penetration of hydrophobic groups into the core of the bilayer.

This picture of PH domain−membrane interactions is more complex than what was suggested initially (*1, 8*) but is consistent with recent NMR data (*25, 68*) and chimeric experiments (*24*) which indicate interactions other than those involving the IP_3-binding site of the protein. Indeed, both the NMR data and our simulations indicate conformational changes in the $\beta5-\beta6$ region upon binding to membranes. Such nonspecific interactions are of special interest given the observation that only 10% of PH domains bind PIs with high affinity (*3*). Here, our focus has been on the PLC$\delta1$ PH domain as this enabled comparison of the experimental and simulation data. Now that the validity of the simulation approach has been demonstrated, it would be interesting to extend it to comparisons with other PH domains.

Of course, these simulations suffer from some technical limitations. The simulations are short relative to a biological time scale and, from the perspective of protein conformational transitions, are likely to be incompletely sampled (*62, 70*). Similarly, simulations of peptide−bilayer interactions suggest time scales of several hundred nanoseconds may be needed for full sampling (*63*). We have in part tried to address this issue via CG simulations, which seem to confirm the global positioning of the PH domain relative to the micelle or bilayer in the atomistic simulations. This suggests that a more general approach might be via multiscale simulations combining CG simulations (to orient the protein) followed by AT simulations (to probe detailed interactions).

A further limitation is the assumption of a fixed ionization state (fully ionized, i.e., charge of −5e) for PIP_2. As noted in ref *48*, the ionization state of PIP_2 could be −3e, −4e, or −5e. Therefore, future studies may use further simulations to more fully explore the effect of varying the ionization state.

A further limitation is the fact that the membranelike environments explored are simplified in terms of their lipid composition. Recent advances in simulations of anionic (*71*) and mixed lipid (*72*) bilayers should allow extension of simulations of interactions of the PH domain with more complex models of cell membranes. Perhaps a more significant extension would be from simulations of an isolated PH domain to simulations of the intact PLC$\delta1$ molecule (which contains PH, EF-hand, catalytic, and C2 domains). However, the results from the current simulations are of sufficient interest to suggest that extension to other domains from signaling proteins which interact with membranes may be of value.

It is interesting to consider the relationship of this study to other simulations of peripheral membrane proteins. A recent simulation study of monotopic membrane enzymes emphasized the role of basic residues in protein−bilayer interactions (*33*). Simulations of the C2 domain of cytosolic phospholipase A2 (*34*) indicate that the C2 domain is able to locally distort the bilayer to optimize its own docking site. This is in agreement with the studies of Cafiso and colleagues which indicate that the Ca^{2+}-binding loops of C2 domains from cPLA2 (*73*) and from synaptotagmin I (*74, 75*) are inserted into the bilayer interior. Thus, it is evident that MD simulations are able to reveal atomic-resolution details of the interactions of peripheral membrane proteins with lipid bilayers. Given the complex multidomain structure of

PLCδ1 (*22, 76*), it therefore would be both interesting and feasible to extend simulations to the intact protein. This would be a first step on the road toward a computational structural biology of membrane-associated protein signaling.

ACKNOWLEDGMENT

Thanks to all of our colleagues for their interest in this work, especially Philip Biggin, Iain Campbell, Philip Fowler, Shozeb Haider, and Michael Overduin.

REFERENCES

1. Cho, W., and Stahelin, R. V. (2005) Membrane-protein interactions in cell signaling and membrane trafficking. *Annu. Rev. Biophys. Biomol. Struct. 34*, 119–151.
2. Bhardwaj, N., Stahelin, R. V., Zhao, G., Cho, W., and Lui, H. (2007) MeTaDoR: A comprehensive resource for membrane targeting domains and their host proteins. *Bioinformatics 23*, 3110–3112.
3. Lemmon, M. A. (2007) Pleckstrin homology (PH) domains and phosphoinositides. *Biochem. Soc. Symp. 74*, 81–93.
4. Lemmon, M. A., Ferguson, K. M., and Abrams, C. S. (2002) Pleckstrin homology domains and the cytoskeleton. *FEBS Lett. 513*, 71–76.
5. Wakelam, M. J. O. (2007) in *Biochemical Society Symposia*, p 277, Portland Press, London.
6. Hyvonen, M., Macias, M. J., Nilges, M., Oschkinat, H., Saraste, M., and Wilmanns, M. (1995) Structure of the binding site for inositol phosphates in a PH domain. *EMBO J. 19*, 4676–4685.
7. Ferguson, K. M., Lemmon, M. A., Schlessinger, J., and Sigler, P. B. (1994) Crystal structure at 2.2 Å resolution of the pleckstrin homology domain from human dynamin. *Cell 79*, 199–209.
8. Ferguson, K. M., Lemmon, M. A., Schlessinger, J., and Sigler, P. B. (1995) Structure of the high affinity complex of inositol trisphosphate with a phospholipase C pleckstrin homology domain. *Cell 83*, 1037–1046.
9. Takenawa, T., and Itoh, T. (2001) Phosphoinositides, key molecules for regulation of actin cytoskeletal organization and membrane traffic from the plasma membrane. *Biochim. Biophys. Acta 1533*, 190–206.
10. Di Paolo, G., and De Camilli, P. (2006) Phosphoinositides in cell regulation and membrane dynamics. *Nature 443*, 651–657.
11. Haider, S., Tarasov, A., Craig, T. J., Sansom, M. S. P., and Ashcroft, F. M. (2007) Identification of the PIP2-binding site on Kir6.2 by molecular modelling and functional analysis. *EMBO J. 26*, 3749–3759.
12. Attree, O., Olivos, I. M., Okabe, I., Bailey, L. C., Nelson, D. L., Lewis, R. A., McInnes, R. R., and Nussbaum, R. L. (1992) The Lowe's oculocerebrorenal syndrome gene encodes a protein highly homologous to inositol polyphosphate-5-phosphatase. *Nature 358*, 239–242.
13. Baraldi, E., Carugo, D. C., Hyvonen, M., Lo Surdo, P., Riley, A. M., Potter, B. V., O'Brien, R., Ladbury, J. E., and Saraste, M. (1999) Structure of the PH domain from Bruton's tyrosine kinase in complex with inositol 1,3,4,5-tetrakisphosphate. *Struct. Folding Des. 7*, 449–460.
14. Clement, S., Krause, U., Desmedt, F., Tanti, J. F., Behrends, J., Pesesse, X., Sasaki, T., Penninger, J., Doherty, M., Malaisse, W., Dumont, J. E., Le Marchand-Brustel, Y., Erneux, C., Hue, L., and Schurmans, S. (2001) The lipid phosphatase SHIP2 controls insulin sensitivity. *Nature 409*, 92–97.
15. Kanai, F., Liu, H., Field, S. J., Akbary, H., Matsuo, T., Brown, G. E., Cantley, L. C., and Yaffe, M. B. (2001) The PX domains of p47phox and p40phox bind to lipid products of phosphoinositide 3-kinase. *Nat. Cell Biol. 3*, 675–678.
16. Rebecchi, M., Peterson, A., and McLaughlin, S. (1992) Phosphoinositide-specific phospholipase Cδ1 binds with high affinity to phospholipid vesicles containing phosphatidylinositol 4,5-bisphosphate. *Biochemistry 31*, 12742–12747.
17. Lemmon, M. A., Ferguson, K. M., O'Brien, R., Sigler, P. B., and Schlessinger, J. (1995) Specific and high-affinity binding of inositol phosphates to an isolated pleckstrin homology domain. *Proc. Natl. Acad. Sci. U.S.A. 92*, 10472–10476.
18. Rhee, S. G. (2001) Regulation of phosphoinositide-specific phospholipase C*. *Annu. Rev. Biochem. 70*, 281–312.
19. Nakahara, M., Shimozawa, M., Nakamura, Y., Irino, Y., Morita, M., Kudo, Y., and Fukami, K. (2005) A novel phospholipase C, PLCη2, is a neuron-specific isozyme. *J. Biol. Chem. 280*, 29128–29134.
20. Renard, D., Poggioli, J., Berthon, B., and Claret, M. (1987) How far does phospholipase C activity depend on the cell calcium concentration? A study in intact cells. *Biochem. J. 243*, 391–398.
21. Thore, S., Wuttke, A., and Tengholm, A. (2007) Rapid turnover of phosphatidylinositol-4,5-bisphosphate in insulin-secreting cells mediated by Ca^{2+} and the ATP-to-ADP ratio. *Diabetes 56*, 818–826.
22. Essen, L. O., Perisic, O., Cheung, R., Katan, M., and Williams, R. L. (1996) Crystal structure of a mammalian phosphoinositide-specific phospholipase Cδ. *Nature 380*, 595–602.
23. Hurley, J. H., and Misra, S. (2000) Signaling and subcellular targeting by membrane-binding domains. *Annu. Rev. Biophys. Biomol. Struct. 29*, 49–79.
24. Varnai, P., Lin, X., Lee, S. B., Tuymetova, G., Bondeva, T., Spat, A., Rhee, S. G., Hajnoczky, G., and Balla, T. (2002) Inositol lipid binding and membrane localization of isolated pleckstrin homology (PH) domains. Studies on the PH domains of phospholipase Cδ1 and p130. *J. Biol. Chem. 277*, 27412–27422.
25. Tuzi, S., Uekama, N., Okada, M., Yamaguchi, S., Saito, H., and Yagisawa, H. (2003) Structure and dynamics of the phospholipase C-δ1 pleckstrin homology domain located at the lipid bilayer surface. *J. Biol. Chem. 278*, 28019–28025.
26. Flesch, F. M., Yu, J. W., Lemmon, M. A., and Burger, K. N. J. (2005) Membrane activity of the phospholipase C-δ1 pleckstrin homology (PH) domain. *Biochem. J. 389*, 435–441.
27. Adcock, S. A., and McCammon, J. A. (2006) Molecular dynamics: Survey of methods for simulating the activity of proteins. *Chem. Rev. 106*, 1589–1615.
28. Ash, W. L., Zlomislic, M. R., Oloo, E. O., and Tieleman, D. P. (2004) Computer simulations of membrane proteins. *Biochim. Biophys. Acta 1666*, 158–189.
29. Roux, B., and Schulten, K. (2004) Computational studies of membrane channels. *Structure 12*, 1343–1351.
30. Nina, M., Bernèche, S., and Roux, B. (2000) Anchoring of a monotopic membrane protein: The binding of prostaglandin H2 synthase-1 to the surface of a phospholipid bilayer. *Eur. Biophys. J. 29*, 439–454.
31. Bemporad, D., Wee, C. L., Sands, Z., Grottesi, A., and Sansom, M. S. P. (2006) VSTx1, a modifier of Kv channel gating, localizes to the interfacial region of lipid bilayers. *Biochemistry 45*, 11844–11855.
32. Wee, C. L., Bemporad, D., Sands, Z. A., Gavaghan, D., and Sansom, M. S. P. (2007) SGTx1, a Kv channel gating-modifier toxin, binds to the interfacial region of lipid bilayers. *Biophys. J. 92*, L07–L09.
33. Fowler, P. W., Balali-Mood, K., Deol, S., Coveney, P. V., and Sansom, M. S. P. (2007) Monotopic enzymes and lipid bilayers: A comparative study. *Biochemistry 46*, 3108–3115.
34. Jaud, S., Tobias, D. J., Falke, J. J., and White, S. H. (2007) Self-induced docking site of a deeply embedded peripheral membrane protein. *Biophys. J. 92*, 517–524.
35. Liepina, I., Czaplewski, C., Janmey, P., and Liwo, A. (2003) Molecular dynamics study of a gelsolin-derived peptide binding to a lipid bilayer containing phosphatidylinositol 4,5-bisphosphate. *Biopolymers 71*, 49–70.
36. Lindahl, E., Hess, B., and van der Spoel, D. (2001) GROMACS 3.0: A package for molecular simulation and trajectory analysis. *J. Mol. Model. 7*, 306–317.
37. van der Spoel, D., Lindahl, E., Hess, B., Groenhof, G., Mark, A. E., and Berendsen, H. J. (2005) GROMACS: Fast, flexible, and free. *J. Comput. Chem. 26*, 1701–1718.
38. van Gunsteren, W. F., Kruger, P., Billeter, S. R., Mark, A. E., Eising, A. A., Scott, W. R. P., Huneberger, P. H., and Tironi, I. G. (1996) *Biomolecular Simulation: The GROMOS96 Manual and User Guide*Biomos & Hochschulverlag AG an der ETH Zurich, Groningen, Germany.
39. Hermans, J., Berendsen, H. J. C., van Gunsteren, W. F., and Postma, J. P. M. (1984) A consistent empirical potential for water-protein interactions. *Biopolymers 23*, 1513–1518.
40. Darden, T., York, D., and Pedersen, L. (1993) Particle mesh Ewald: An N.log(N) method for Ewald sums in large systems. *J. Chem. Phys. 98*, 10089–10092.
41. Essmann, U., Perera, L., Berkowitz, M. L., Darden, T., Lee, H., and Pedersen, L. G. (1995) A smooth particle mesh Ewald method. *J. Chem. Phys. 103*, 8577–8593.

42. Berendsen, H. J. C., Postma, J. P. M., van Gunsteren, W. F., DiNola, A., and Haak, J. R. (1984) Molecular dynamics with coupling to an external bath. *J. Chem. Phys. 81*, 3684–3690.
43. Hess, B., Bekker, H., Berendsen, H. J. C., and Fraaije, J. G. E. M. (1997) LINCS: A linear constraint solver for molecular simulations. *J. Comput. Chem. 18*, 1463–1472.
44. Goodsell, D. S., Morris, G. M., and Olson, A. J. (1996) Automated docking of flexible ligands: Applications of AutoDock. *J. Mol. Recognit. 9*, 1–5.
45. Humphrey, W., Dalke, A., and Schulten, K. (1996) VMD: Visual Molecular Dynamics. *J. Mol. Graphics 14*, 33–38.
46. Sayle, R. A., and Milner-White, E. J. (1995) RasMol: Biomolecular graphics for all. *Trends Biochem. Sci. 20*, 374–376.
47. van Aalten, D. M., Bywater, R., Findlay, J. B., Hendlich, M., Hooft, R. W., and Vriend, G. (1996) PRODRG, a program for generating molecular topologies and unique molecular descriptors from coordinates of small molecules. *J. Comput.-Aided Mol. Des. 10*, 255–262.
48. McLaughlin, S., Wang, J., Gambhir, A., and Murray, D. (2002) PIP_2 and proteins: Interactions, organization, and information flow. *Annu. Rev. Biophys. Biomol. Struct. 31*, 151–175.
49. Bond, P. J., Cuthbertson, J. M., Deol, S. D., and Sansom, M. S. P. (2004) MD simulations of spontaneous membrane protein/detergent micelle formation. *J. Am. Chem. Soc. 126*, 15948–15949.
50. Tieleman, D. P., and Berendsen, H. J. C. (1996) Molecular dynamics simulations of a fully hydrated dipalmitoylphosphatidycholine bilayer with different macroscopic boundary conditions and parameters. *J. Chem. Phys. 105*, 4871–4880.
51. Bond, P. J., and Sansom, M. S. P. (2003) Membrane protein dynamics vs. environment: Simulations of OmpA in a micelle and in a bilayer. *J. Mol. Biol. 329*, 1035–1053.
52. Lazaridis, T., Mallik, B., and Chen, Y. (2005) Implicit solvent simulations of DPC micelle formation. *J. Phys. Chem. B 109*, 15098–15106.
53. Marrink, S. J., de Vries, A. H., and Mark, A. E. (2004) Coarse grained model for semiquantitative lipid simulations. *J. Phys. Chem. B 108*, 750–760.
54. Bond, P. J., and Sansom, M. S. P. (2006) Insertion and assembly of membrane proteins via simulation. *J. Am. Chem. Soc. 128*, 2697–2704.
55. Bond, P. J., Holyoake, J., Ivetac, A., Khalid, S., and Sansom, M. S. P. (2007) Coarse-grained molecular dynamics simulations of membrane proteins and peptides. *J. Struct. Biol. 157*, 593–605.
56. Scott, K. A., Bond, P. J., Ivetac, A., Chetwynd, A. P., Khalid, S., and Sansom, M. S. P. (2008) Coarse-grained MD simulations of membrane protein/bilayer self assembly. *Structure* (in press).
57. Bromann, P. A., Boetticher, E. E., and Lomasney, J. W. (1997) A single amino acid substitution in the pleckstrin homology domain of phospholipase Cδ1 enhances the rate of substrate hydrolysis. *J. Biol. Chem. 272*, 16240–16246.
58. Kutateladze, T., and Overduin, M. (2001) Structural mechanism of endosome docking by the FYVE domain. *Science 291*, 1793–1796.
59. Dancea, F., Kami, K., and Overduin, M. (2008) Lipid interaction networks of peripheral membrane proteins revealed by data-driven micelle docking. *Biophys. J. 94*, 515–524.
60. Pang, A., Arinaminpathy, Y., Sansom, M. S. P., and Biggin, P. C. (2003) Interdomain dynamics and ligand binding: Molecular dynamics simulations of glutamine binding protein. *FEBS Lett. 550*, 168–174.
61. Fan, H., and Mark, A. E. (2003) Relative stability of protein structures determined by X-ray crystallography or NMR spectroscopy: A molecular dynamics simulation study. *Proteins: Struct., Funct., Bioinf. 53*, 111–120.
62. Grossfield, A., Feller, S. E., and Pitman, M. C. (2007) Convergence of molecular dynamics simulations of membrane proteins. *Proteins: Struct., Funct., Bioinf. 67*, 31–40.
63. Babakhani, A., Gorfe, A. A., Gullingsrud, J., Kim, J. E., and McCammon, J. A. (2007) Peptide insertion, positioning, and stabilization in a membrane: Insight from an all-atom molecular dynamics simulation. *Biopolymers 85*, 490–497.
64. Gorfe, A. A., Hanzal-Bayer, M., Abankwa, D., Hancock, J. F., and McCammon, J. A. (2007) Structure and dynamics of the full-length lipid-modified H-Ras protein in a 1,2-dimyristoylglycero-3-phosphocholine bilayer. *J. Med. Chem. 50*, 674–684.
65. Ohkubo, Y. Z., and Tajkhorshid, E. (2008) Distinct structural and adhesive roles of Ca^{2+} in membrane binding of blood coagulation factors. *Structure 16*, 72–81.
66. Periole, X., Huber, T., Marrink, S. J., and Sakmar, T. P. (2007) G protein-coupled receptors self-assemble in dynamics simulations of model bilayers. *J. Am. Chem. Soc. 129*, 10126–10132.
67. Sansom, M. S. P., Scott, K. A., and Bond, P. J. (2008) Coarse grained simulation: A high throughput computational approach to membrane proteins. *Biochem. Soc. Trans. 36*, 27–32.
68. Uekama, N., Sugita, T., Okada, M., Yagisawa, H., and Tuzi, S. (2007) Phosphatidylserine induces functional and structural alterations of the membrane-associated pleckstrin homology domain of phospholipase C-δ1. *FEBS J. 274*, 177–187.
69. Gryk, M. R., Abseher, R., Simon, B., Nilges, M., and Oschkinat, H. (1998) Heteronuclear relaxation study of the PH domain of β-spectrin: Restriction of loop motions upon binding inositol trisphosphate. *J. Mol. Biol. 280*, 879–896.
70. Faraldo-Gómez, J. D., Forrest, L. R., Baaden, M., Bond, P. J., Domene, C., Patargias, G., Cuthbertson, J., and Sansom, M. S. P. (2004) Conformational sampling and dynamics of membrane proteins from 10-ns computer simulations. *Proteins: Struct., Funct., Bioinf. 57*, 783–791.
71. Mukhopadhyay, P., Monticelli, L., and Tieleman, D. P. (2004) Molecular dynamics simulation of a palmitoyl-oleoyl phosphatidylserine bilayer with Na^+ counterions and NaCl. *Biophys. J. 86*, 1601–1609.
72. Bhide, S. Y., Zhang, Z., and Berkowitz, M. L. (2007) Molecular dynamics simulations of SOPS and sphingomyelin bilayers containing cholesterol. *Biophys. J. 92*, 1284–1295.
73. Frazier, A. A., Wisner, M. A., Malmberg, N. J., Victor, K. G., Fanucci, G. E., Nalefski, E. A., Falke, J. J., and Cafiso, D. S. (2002) Membrane orientation and position of the C2 domain from cPLA2 by site-directed spin labeling. *Biochemistry 41*, 6282–6292.
74. Frazier, A. A., Roller, C. R., Havelka, J. J., Hinderliter, A., and Cafiso, D. S. (2003) Membrane-bound orientation and position of the synaptotagmin I C2A domain by site-directed spin labeling. *Biochemistry 42*, 96–105.
75. Rufener, E., Frazier, A. A., Wieser, C. M., Hinderliter, A., and Cafiso, D. S. (2005) Membrane-bound orientation and position of the synaptotagmin C2B domain determined by site-directed spin labeling. *Biochemistry 44*, 18–28.
76. Essen, L. O., Perisic, O., Lynch, D. E., Katan, M., and Williams, R. L. (1997) A ternary metal binding site in the C2 domain of phosphoinositide-specific phospholipase C-δ1. *Biochemistry 36*, 2753–2762.

BI702319K